# Three-Dimensional Electrically Interconnected Nanowire Networks Formed by Diffusion Bonding

Zhiyong Gu,[†,||] Hongke Ye,[†] Adam Bernfeld,[†] Kenneth J. T. Livi,[‡] and David H. Gracias*[,†,§]

*Department of Chemical and Biomolecular Engineering, Morton K. Blaustein Department of Earth & Planetary Sciences, and Department of Chemistry, Johns Hopkins University, 3400 N Charles Street, Baltimore, Maryland 21218*

*Received September 25, 2006. In Final Form: December 7, 2006*

We demonstrate a new strategy to bond nanowires (NWs) using diffusion bonding of gold (Au). The strategy was used to form very large scale, electrically interconnected 3D NW networks composed of both homogeneous and heterogeneous (multisegmented) NWs. The size of the networks ranged from tens of micrometers to millimeters. We have measured the electrical characteristics of the networks and explored one application of the networks in 3D spatial chemical sensing.

We explored the use of diffusion bonding (DB) to form metallic (low-resistance) contacts between nanoscale components. DB is a well-established method for permanently joining macroscale components to form robust metal−metal, metal−semiconductor, and metal−ceramic joints.[1−4] Au is an attractive metal for DB because of its low modulus, rapid self-diffusion, and the absence of oxide formation on heating.[5] Gold DB is typically carried by bringing components (with clean Au interfaces) together at elevated temperatures and pressures. In the absence of elevated pressures, high temperatures above ∼430 °C are required[5] to get appreciable Au diffusion to bind Au−Au interfaces. This requirement of high temperature or elevated pressure restricts the utility of DB because most electronic, photonic, and biomedical devices are processed at relatively low temperatures and ambient pressures.

One path to facilitate DB at lower temperatures and ambient pressure is to increase the atomic diffusion rate of Au using chemical methods. The enhanced diffusion of gold in strong acids[6−9] has been utilized in other applications such as the formation of nanoporous Au.[6,9] We observed significant surface diffusion of Au even in milder organic acids (such as palmitic acid) at relatively low temperatures (∼230−270 °C) and ambient pressure. Using this diffusing layer at Au interfaces, we investigated the possibility of DB for nanowires (NWs) containing Au segments to form large-scale 3D networks in a fluidic medium at relatively low temperature and ambient pressure (i.e., a relatively milder and more versatile DB process that can be carried out in a solvent). We fabricated single and multisegment NWs (diameters 30−200 nm, lengths 1−5 $\mu$m) using electrodeposition in nanoporous templates[10] as described before.[11] Diffusion bonding was carried out by heating the NWs in relatively high-boiling-point solvents (*N*-methylpyrrolidione (NMP) or triethylene glycol (TEG)) into which was dissolved an organic acid. The NWs with Au diffusing at the surface of Au segments bonded with each other, after coalescing as a result of convective currents and interfacial and van der Waals forces, and we observed the formation of aggregated networks in solution (Supporting Information). After being heated for about 20 min, the samples were cooled. The solvent was replaced with ethanol, and then the aggregates were rinsed repeatedly and characterized using electron and optical microscopy. From the scanning electron microscopy (SEM) images (Figure 1), it is evident that the surfaces of the NWs were modified during the heating process, with Au diffusing between NWs to form well-connected joints. The interfacial diffusion was large enough to alter the shape of 30 nm nominal diameter NWs (Figure 1c) significantly, with certain sections of the NWs thickening at the expense of others, producing a sausagelike shape. The extent of diffusion could be controlled to some extent; the diffusion increased with increasing temperature and time.

The DB worked best with an organic solder flux (which contains several organic acids such as abietic acid) as the acid and NMP as the solvent and at temperatures in the range of ∼230−270 °C (smaller-diameter NWs required a relatively lower temperature). Au diffusion was also significant in the presence of strong inorganic acids (e.g., 70% $HNO_3$), but the assembled aggregates were smaller and contained fewer NWs. In the absence of any acid, no obvious change was observed in the NWs upon heating to 270 °C.

Figure 2 shows transmission electron microscopy (TEM) images of 50 nm nominal diameter Au NWs on a holey carbon grid before (Figure 2a−c) and after (Figure 2d−f) NW DB. From the dark-field image in Figure 2b, we observe that NWs before DB are composed primarily of a large number of small crystals (individual crystals in the proper diffracting condition are bright in dark-field images), which is typical of polycrystalline electrodeposited NWs.[10] After DB, the NWs were composed of fewer but larger crystals. (Note the small number of relatively large crystals that are bright in Figure 2e.) The selected-area

* Corresponding author. E-mail: dgracias@jhu.edu.
† Department of Chemical and Biomolecular Engineering.
‡ Morton K. Blaustein Department of Earth & Planetary Sciences.
§ Department of Chemistry.
|| Current address: Department of Chemical Engineering and UML Nanomanufacturing Center of Excellence, University of Massachusetts Lowell, Lowell, MA 01854.

(1) Ornellas, D. L.; Catalano, E. *Rev. Sci. Instrum.* **1974**, *45*, 955.
(2) Kazakov, N. F. *Diffusion Bonding of Materials*; Pergamon Press: Oxford, U.K., 1985.
(3) Tsau, C. H.; Spearing, S. M.; Schmidt, M. A. *J. Microelectromech. Syst.* **2002**, *11*, 641−647.
(4) Mosley, D. W.; Chow, B. Y.; Jacobson, J. M. *Langmuir* **2006**, *22*, 2437−2440.
(5) Humpston, G.; Baker, S. J. *Gold Bull.* **1998**, *31*, 131−133.
(6) Erlebacher, J.; Aziz, M. J.; Karma, A.; Dimitrov, N.; Sieradzki, K. *Nature* **2001**, *410*, 450−453.
(7) Ikemiya, N.; Nishide, M.; Hara, S. *Surf. Sci.* **1995**, *340*, L965−L970.
(8) Dona, J. M.; Velasco, J. G. *J. Phys. Chem.* **1993**, *97*, 4714−4719.
(9) Mohamed, M. B.; Wang, Z. L.; El-Sayed, M. A. *J. Phys. Chem. A* **1999**, *103*, 10255−10259.
(10) Martin, C. R. *Science* **1994**, *266*, 1961−1966.
(11) Gu, Z.; Ye, H.; Smirnova, D.; Small, D.; Gracias, D. H. *Small* **2006**, *2*, 225−229.

10.1021/la062813s CCC: $37.00 
Published on Web 12/23/2006

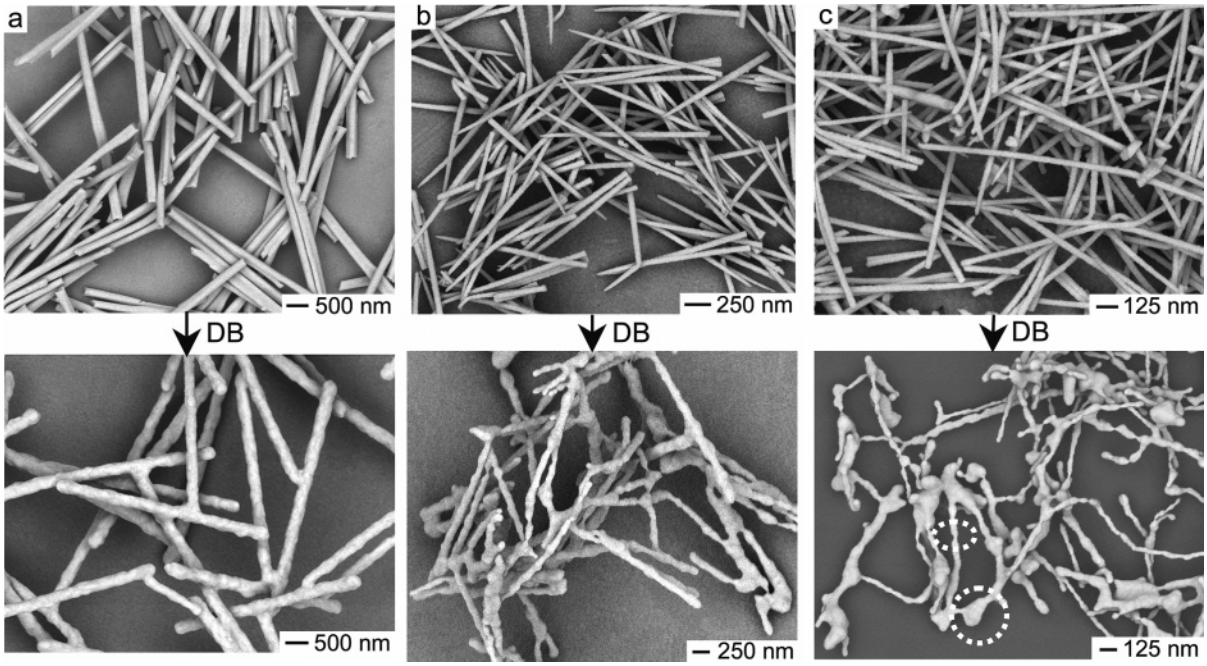


**Figure 1.** Diffusion bonding of (a) 200, (b) 50, and (c) 30 nm nominal diameter Au NWs. The SEM images in the upper row are as-electrodeposited, pristine Au NWs, and those in the lower row are NWs that were subjected to the fluidic DB process. Surface diffusion of Au, upon heating, is evident and was large enough to alter the shape of the 30 nm NWs significantly. The circled regions in c show thin and thick regions formed within the 30 nm NW networks after DB, forming a sausagelike texture.

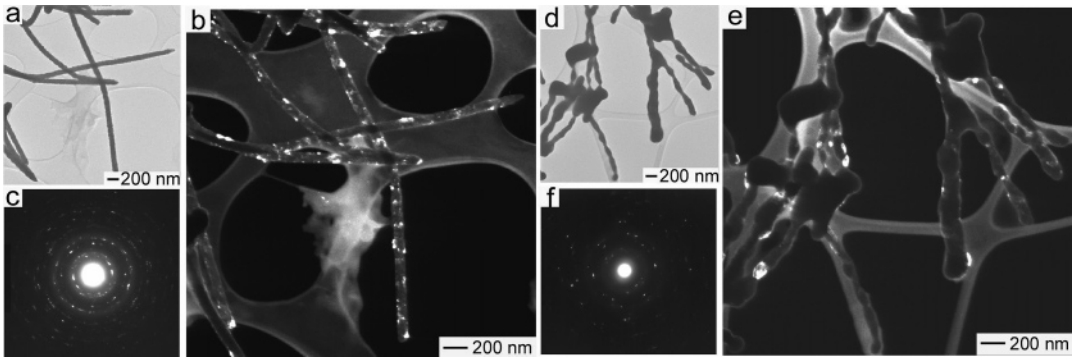


**Figure 2.** TEM images of 50 nm nominal diameter Au NWs (a−c) before and (d−f) after diffusion bonding. (a, d) Bright-field, (b, e) dark-field, and (c, f) SAED patterns. From the images, we can conclude that the diffusion mechanism is associated with the growth of larger crystals at the expense of smaller ones within Au nanowires.

electron diffraction (SAED) pattern of NWs (Figure 2f) after DB had fewer diffraction spots and less-complete rings as compared to that observed in NWs before DB (Figure 2c), which implies fewer crystals after DB. Hence, the TEM analysis (dark-field and SAED) suggests a diffusion mechanism in which larger Au crystals grow at the expense of smaller ones, reminiscent of Ostwald ripening.[12]

As opposed to selective etching and solution- or vapor-phase growth of NW networks, our strategy facilitates the fabrication of both homogeneous (composed of NWs with one segment material) as well as heterogeneous (composed of NWs with more than one segment material) 3D networks. The possibility of fabricating 3D networks with multisegmented NWs represents an attractive strategy for the fabrication of functional 3D interconnected devices with considerable complexity because multisegmented NWs can function as basic electronic circuit elements (e.g., diodes[13]). It should be noted that the strategy that we have demonstrated results in the formation of random networks, and it may also be necessary to structure the components prior to DB to facilitate increased network complexity and functionality. Devices with large numbers of components, highly interconnected in all three dimensions, have advantages: (a) high interconnectivity allows device integration with shorter interconnects, increases defect tolerance, and facilitates architectures for neuromorphic computing; (b) a higher surface area-to-volume ratio increases the extent of interactions with the surrounding medium; and (c) higher packing densities allows the fabrication of devices with small factors. At the present time, however, these 3D highly interconnected electrical devices remain largely unexplored as a result of the inherent two dimensionality of photolithography that prohibits large-scale integration in all three dimensions. Self-assembly is one attractive methodology to facilitate connections between NWs in all three dimensions. However, present day bonding strategies used in self-assembly including the use of molecular linkers,[14,15] biological organisms,[16]

(12) Ostwald, W. *Z. Phys. Chem.* **1901**, *37*, 385.
(13) Park, S.; Chung, S.-W.; Mirkin, C. A. *J. Am. Chem. Soc.* **2004**, *126*, 11772−11773.
(14) Mirkin, C. A. *Inorg. Chem.* **2000**, *39*, 2258−2272.
(15) Mbindyo, J. K. N.; Reiss, B. D.; Martin, B. R.; Keating, C. D.; Natan, M. J.; Mallouk, T. E. *Adv. Mater.* **2001**, *13*, 249−254.

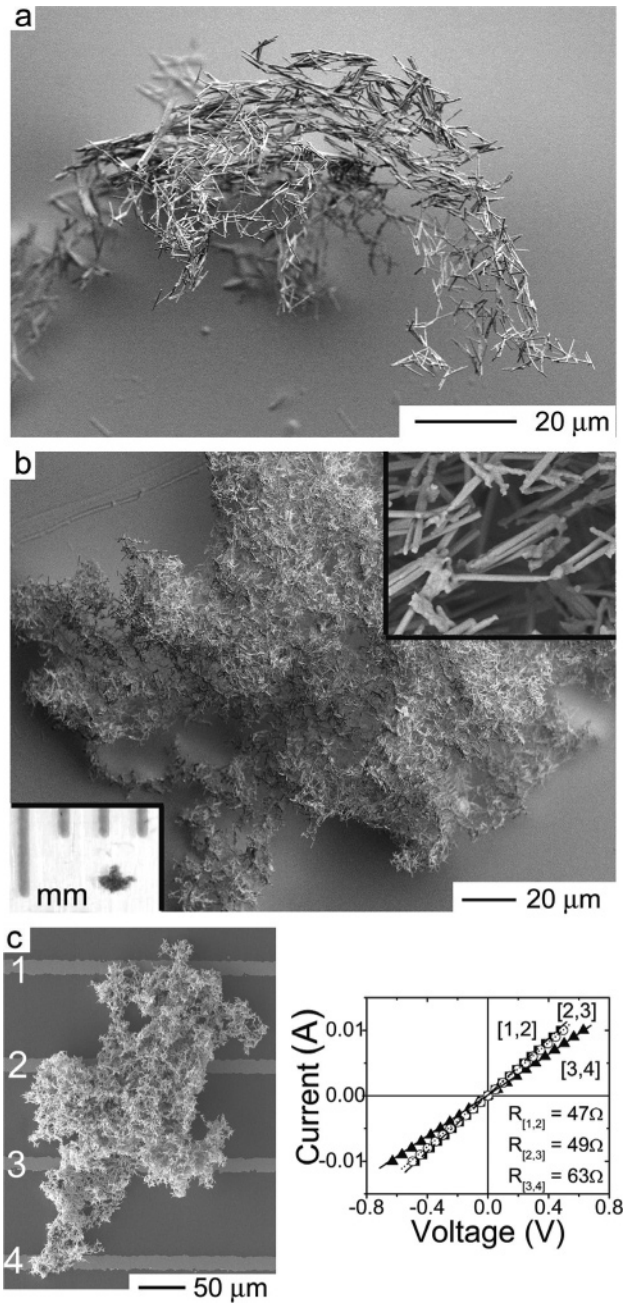


**Figure 3.** (a) SEM image of a 100-$\mu$m-scale 3D Au NW network. (b) SEM image of a very large scale 3D Au−Pt−Au NW network; one inset shows that networks as large as 1 mm can be formed, and the other inset is an enlarged image of the network showing that the primary mode of connection between adjacent NWs is through the Au tips. (c) SEM image of a 3D Au−Pt−Au NW network on microfabricated contact pads. Also shown are the current−voltage curves measured across contact pads [1, 2], [2, 3], and [3, 4].

capillary interactions,[17,18] and electrostatic forces[19,20] result in high electrical resistance interconnections between components.

We assembled large-scale homogeneous NW networks with pure Au NWs (Figure 3a). Heterogeneous NW networks were assembled from multisegmented NWs containing gold and

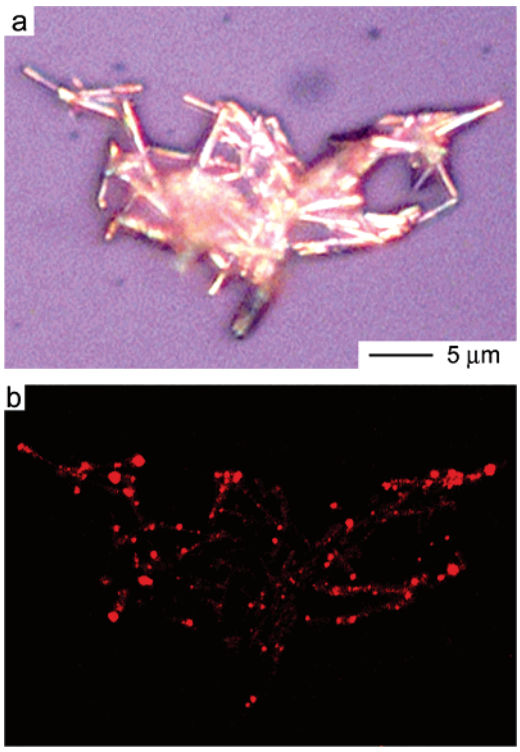


**Figure 4.** One application of the 3D networks as a scaffold for the 3D chemical sensing of an analyte. (a, b) Bright-field and fluorescent confocal images of an Au−Pt−Au 3D NW network exposed to 1-butaneisocyanide, cyestamine (MEA), and rhodamine B isothiocyanate. The 3D red fluorescent map represents regions where rhodamine B is bonded to cyestamine that adsorbs primarily on the Au segments within the NW network. The fluorescence image thus maps the concentration of MEA in 3D. The fluorescence observed primarily at the tips of the interconnected network also confirmed that the primary mode of connectivity in the heterogeneous Au−Pt−Au network was between Au segments.

platinum. (Platinum is widely used in catalysis and sensing.) When segmented Au−Pt−Au NWs were heated in the acidic medium, the Pt segments were unaffected and the Au diffused at the interfaces of Au segments, as expected. Large networks composed of the multisegmented NWs were observed (Figure 3b). Within the networks, the primary mode of connectivity was between Au head and tail segments (inset in Figure 3b). Depending on the number of NWs used in the assembly process and the volume of the container in which the assembly was carried out, networks could be formed with sizes ranging from micrometers to millimeters (Figure 3b).

We used electrical probing on 2D contact pads (across which NW networks were deposited) to measure the current−voltage ($I-V$) characteristics of the 3D NW networks. It was possible to deposit the networks directly on contact pads (followed by thermal annealing at 300 °C for 30 min in air, Figure 3c) or pattern contact pads on top of the networks using photolithographic lift-off. With either type of contact pad and for both pure Au as well as Au−Pt−Au networks, the $I-V$ curves were ohmic, with electrical resistances ranging from 5 to 200 Ω for 200-nm-diameter NW networks; the characteristic size scale of the networks used for these electrical measurements ranged from tens to hundreds of micrometers. We were also able to measure the $I-V$ curves across different regions of the same network (Figure 3c). The consistently ohmic, low resistances measured are consistent with electron microscopy images that show Au diffusion at the interfaces of adjacent NW segments and the formation of fused metallic contacts between NWs.

(16) Nam, K. T.; Kim, D.-W.; Yoo, P. J.; Chiang, C.-Y.; Meethong, N.; Hammond, P. T.; Chiang, Y.-M.; Belcher, A. M. *Science* **2006**, *312*, 885−888.
(17) Terfort, A.; Bowden, N.; Whitesides, G. M. *Nature* **1997**, *386*, 162−164.
(18) Gu, Z.; Chen, Y.; Gracias, D. H. *Langmuir* **2004**, *20*, 11308−11311.
(19) Kalsin, A. M.; Fialkowski, M.; Paszewski, M.; Smoukov, S. K.; Bishop, K. J. M.; Grzybowski, B. A. *Science* **2006**, *312*, 420−424.
(20) Jacobs, H. O.; Campbell, S. A.; Steward, M. G. *Adv. Mater.* **2002**, *14*, 1553−1557.

We foresee several immediate applications for 3D NW networks as electromagnetic shields, scaffolds for tissue engineering, 3D porous supports for catalysis, electrode surfaces for fuel cells, and substrates for 3D surface-enhanced Raman scattering (SERS). We also believe that 3D networks, as a result of their high surface area-to-volume ratio, are attractive devices for 3D chemical sensing because the 3D network can be chemically functionalized to map the concentration of a chemical spatially in 3D using an electrical or optical response. To demonstrate 3D sensing, we treated a network composed of Au−Pt−Au NWs with 1 mL of 1 mM butaneisocyanide (BIC) and allowed it to react for 18 h while the solution was shaken using a vortex mixer; the BIC molecules bind all over the NW network. The network was rinsed thoroughly with hexane and ethanol to remove any unbound BIC. The 3D network was subsequently exposed to an analyte, 1 mL of 1 mM cysteamine (a thiol amine, MEA). The MEA displaced the BIC molecules only on the Au segments (forming a Au−thiol linkage). The NWs were repeatedly washed with ethanol and finally stored in nitrogen-bubbled ethanol. Subsequently, a fluorescent reporter molecule (rhodamine B isothiocyanate) (2 mg/1 mL nitrogen-bubbled ehtanol) was then added, and the solution was shaken for 18 h. Rhodamine B that binds only to the amine group of MEA[21] allowed us to detect MEA optically and obtain a 3D map of the binding of MEA on the network. The 3D Au−Pt−Au NW networks (Figure 4a) fluoresced (Figure 4b) primarily at the Au tips and junctions, and it was possible to get a 3D spatial map of MEA along the NW network using confocal microscopy. The fluorescence primarily at the tips of the interconnected network also confirmed that the primary mode of connectivity in the heterogeneous Au−Pt−Au network was between Au segments.

(21) Martin, B. R.; Dermody, D. J.; Reiss, B. D.; Fang, M.; Lyon, L. A.; Natan, M. J.; Mallouk, T. E. *Adv. Mater.* **1999**, *11*, 1021−1025.

In summary, we have demonstrated a general strategy based on DB in a fluidic medium to construct very large scale electrically interconnected homogeneous and heterogeneous metallic NW networks. The fluidic DB strategy is versatile and can be used to bond any arbitrary nanoparticle containing Au. (See Figure 3 in Supporting Information for the bonding of spherical Au nanoparticles.) The size of the networks can be engineered from a small size scale (tens of NWs) to a very large size scale (millions of NWs). In the future, the functional complexity of the 3D networks can be increased by utilizing multisegmented-NW-based semiconductor or optical elements (with Au contacts) as building blocks and/or selectively functionalizing heterogeneous 3D networks after assembly.

**Acknowledgment.** We acknowledge funding support from the National Science Foundation Career Award (DMI− 0448816), the NSF-IIS, and the American Chemical Society Petroleum Research Fund (ACS-PRF). The Johns Hopkins University Electron Microbeam Facility was established through grants from the Keck Foundation and the NSF. The views expressed herein are not necessarily endorsed by the sponsors.

**Supporting Information Available:** Experimental details of NW fabrication, diffusion bonding of NWs, characterization using electron microscopy, electrical characterization of NW networks, and sensing experiments. Plots of indexed SAED patterns from Figure 2c,f, results of a control experiment showing preferential binding of MEA at the tips of untreated Au−Pt−Au NWs, and the strategy of fluidic DB applied to Au nanoparticles. This material is available free of charge via the Internet at http://pubs.acs.org.

LA062813S

## Experimental Details

### NW Fabrication

The strategy used to fabricate segmented NWs has been discussed in detail before (Z. Gu, H. Ye, D. Smirnova, D. Small and D. H. Gracias, *"Reflow and Electrical Characteristics of Nanoscale solder"*, Small (2006), 2, 2, 225-229). Briefly it involved the electrodeposition of metals in nanoporous templates. First, a 200 nm Silver (Ag, Alfa Aesar, 99.99%, www.alfa.com) layer was evaporated in a thermal evaporator on one side of a commercial alumina or polycarbonate membrane (Whatman, www.whatman.com). The membrane was placed in contact with a copper plate, and restrained using a glass joint and viton o-ring seal. The membrane was soaked in water for 5-20 minutes, (depending on the pore size of the membranes) and then filled with the electrolytic solution of choice. We used commercial plating solutions for Ag (Techni Silver E-2, Technic. Inc, www.technic.com), Au (Techni Gold 25E), Pt (Techni Platinum TP solution). Typical electrodeposition conditions were 0.8 to 3.3 $mA/cm^2$ for Ag, Au, and Pt. The membrane was washed several times with water between each electrodeposition.

After electrodeposition, the Ag seed layer on one side of the alumina membrane was dissolved in 6M $HNO_3$ and the membrane was dissolved in 2 M NaOH. After membrane dissolution was complete, the NaOH was removed by centrifugation at 5000-6000 rpm for 5-6 minutes, and the wires were rinsed repeatedly with water and ethanol and then stored in ethanol. In the case of polycarbonate membranes, the NWs were released from the membrane by dissolving the entire membrane in methylene chloride. The NWs were repeatedly rinsed in methylene chloride and then stored in ethanol.

**Diffusion Bonding of NWs**

The DB worked best with an organic solder flux (which contains several organic acids such as abietic acid) as the acid and NMP as the solvent, and at temperatures in the range of ~230-270°C. About 5mg RMA flux (Indium Corporation, www.indium.com) was added into 0.5mL NMP (Aldrich, www.sigmaaldrich.com, boiling point 202 °C). The NMP solution was preheated to 120 °C for about 5min, and then 4-5 drops of the NW suspension (in ethanol) were added to the NMP solution. The mixture was heated to 150 °C for 5 min to completely evaporate the ethanol. The temperature was then increased to 200-220 °C for 10min, at which point NMP convective currents were observed and provided good agitation for the NW assembly. Finally, the temperature was raised to 230-270 °C for 10min to ensure sufficient Au surface diffusion. It was also possible to use other high boiling point solvents, such as triethylene glycol anhydrous (Fluka, www.sigmaaldrich.com,.boiling point 285 °C) as well as other organic acids, like palmitic acid (Aldrich, www.sigmaaldrich.com) for diffusion bonding of NWs.

**Characterization Using Electron Microscopy**

SEM images were taken on a JEOL JSM-6700F Field-Emission Scanning Electron Microscope operated at 10 kV. The networks in ethanol were pipetted onto a silicon or metal-coated silicon support, and the solvent was allowed to evaporate. TEM images were taken with a Philips CM300 FEG operating at 297 kV. NW particles and networks were triple-rinsed in nano-pure water and deposited onto holey carbon grids. Dark-field images for both samples were formed using an objective aperture with a 0.3 $Å^{-1}$ radius over the 111* ring. SAED patterns were collected using the same selected area aperture with a projected radius of 0.8 μm. Bright-field and dark-field images were collected on a

Gatan GIF 200 Multiscan CCD camera. SAED patterns were collected on film.

**Electrical Characterization of the NW Networks**

The resistance of NW networks was measured using a Keithley 2400 digital source meter across adjacent contact pads. The I–V curves were obtained using the source meter by scanning the current from -10 to 10 mA. Every network was measured three times and a reproducible ohmic response was observed.

**Sensing Experiments**

Individual Au-Pt-Au NWs: About 0.1 mL of the NW suspension in hexane was added to 1 mL of 1 mM 1-butaneisocyanide (BIC, Acros Organics, www.acros.com) and allowed to react for 18 h, while the solution was shaken using a vortex mixer. The NWs were collected and rinsed using 5 centrifugation/resuspension cycles with hexane and then 1 cycle with ethanol. The NWs were resuspended by brief sonication in ethanol. This suspension was added to 1 mL of 1 mM 2-mercaptoethylamine (MEA, Aldrich) and was allowed to react for 18 h. The MEA displaces the BIC from the Au segments, but not from Pt segments. The NWs were repeatedly washed with ethanol, and finally stored in nitrogen-bubbled ethanol. Rhodamine B isothiocyanate (Aldrich) (2mg/1mL nitrogen-bubbled ehtanol) was then added, and the solution was shaken for 18 h. The NWs were rinsed repeatedly (~10 times) with ethanol. A drop of the resuspended NWs was placed on a Petri dish (with a quartz microscope slide), and allowed to dry for fluorescent imaging.

Sensing with Au-Pt-Au NW networks: NW networks were sequentially exposed to BIC, MEA, and Rhodamine as detailed above. However the centrifugation and sonication steps were skipped, as vigorous agitation and centrifuge damage the networks.

Fluorescent images were taken on a Zeiss Axiovert inverted light microscope equipped with excitation and emission filter wheels; confocal images were taken on a Zeiss LSM 510 META Confocal (Johns Hopkins University Integrated Imaging Center).

**Supplementary Figures**

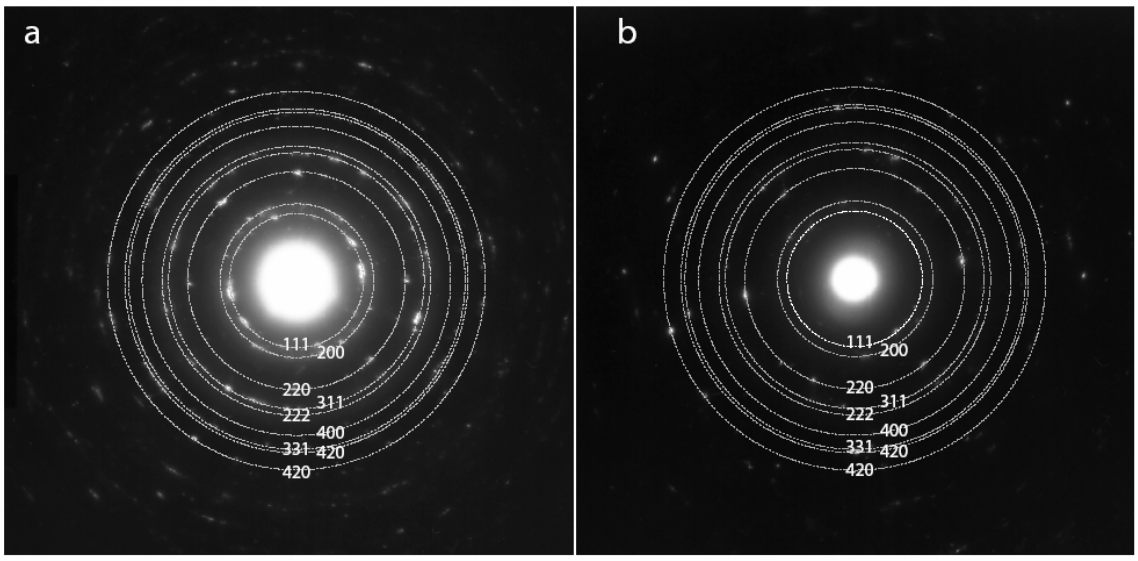


**Fig. 1**: Indexed SAED patterns from Fig. 2c & f. Indexing was done for the Au fcc structure, a) before treatment (indexed version of Fig. 2c) and, b) after treatment (indexed version of Fig. 2f).

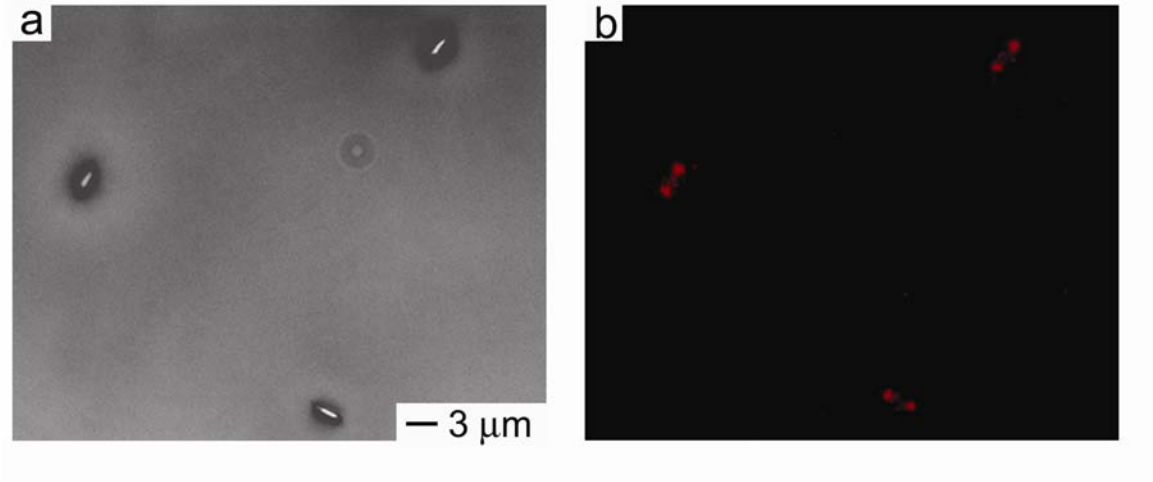


**Fig. 2:** Results of a control experiment showing preferential binding of MEA at the tips of untreated Au-Pt-Au NWs. This is readily seen in the fluorescence images (the fluorescent functionalized rhodamine reporter binds only to MEA); the NWs fluoresce predominantly at the Au tips.

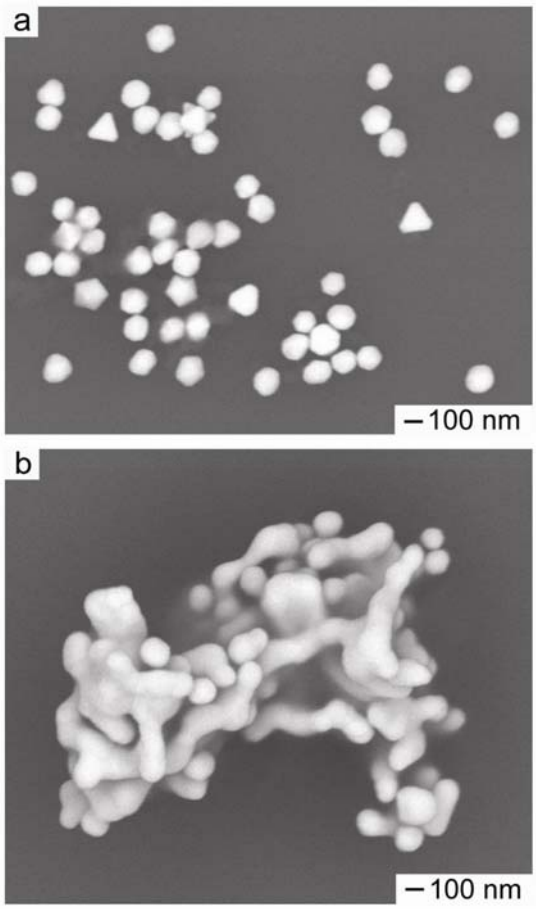


**Fig 3:** Our strategy of fluidic DB is versatile and can be used to bond any arbitrary nanoparticle. The SEM images above show the bonding of Au nanoparticles to form an interconnected network.